The dynamics of engineered resident proteins in the mammalian Golgi complex relies on cisternal maturation

Riccardo Rizzo,[1,2] Seetharaman Parashuraman,[1,2] Peppino Mirabelli,[3] Claudia Puri,[2] John Lucocq,[4] and Alberto Luini[1,2]

[1]Instituto di Biochimica delle Proteine, Consiglio Nazionale delle Richerche, 80131 Naples, Italy
[2]Telethon Institute of Genetics and Medicine, 80131 Naples, Italy
[3]Istituto di Ricovero e Cura a Carattere Scientifico-SDN, 80143 Naples, Italy
[4]School of Medicine, University of St. Andrews, St. Andrews, Fife KY16 9TF, Scotland, UK

After leaving the endoplasmic reticulum, secretory proteins traverse several membranous transport compartments before reaching their destinations. How they move through the Golgi complex, a major secretory station composed of stacks of membranous cisternae, is a central yet unsettled issue in membrane biology. Two classes of mechanisms have been proposed. One is based on cargo-laden carriers hopping across stable cisternae and the other on "maturing" cisternae that carry cargo forward while progressing through the stack. A key difference between the two concerns the behavior of Golgi-resident proteins. Under stable cisternae models, Golgi residents remain in the same cisterna, whereas, according to cisternal maturation, Golgi residents recycle from distal to proximal cisternae via retrograde carriers in synchrony with cisternal progression. Here, we have engineered Golgi-resident constructs that can be polymerized at will to prevent their recycling via Golgi carriers. Maturation models predict the progress of such polymerized residents through the stack along with cargo, but stable cisternae models do not. The results support the cisternal maturation mechanism.

Introduction

After synthesis in the ER, cargo proteins reach and traverse the Golgi complex, an organelle that is composed of stacks of membranous cisternae where cargo is modified by glycosylating enzymes during transport. The mechanism of intra-Golgi transport has been studied for decades and most if not all of the possible avenues of investigation have been documented or hypothesized. It is fair to say, however, that transport through the Golgi remains one of the main unsettled questions in membrane biology (Pfeffer, 2007). There are two types of transport models, with one based on stable cisternae, and the other on "maturing" cisternae. Under the stable cisternae models, cisternae never change their molecular composition and location in the stack, and secretory cargo is transported forward from one cisterna to the next via vesicles or other intermediates (Rothman and Wieland, 1996; Patterson et al., 2008; Pfeffer, 2010). According to the maturation model, instead, new cargo-containing cisternae continuously form at the cis-Golgi face and progress toward the trans face while changing their composition (i.e., maturing) through the recycling of resident enzymes via retrograde vesicles or tubules, in synchrony with cisternal progression. Upon reaching the trans-most position, the cargo-laden cisternae disassemble into anterograde carriers (Nakano and Luini, 2010; Glick and Luini, 2011). A role for this mechanism in mammals is supported by the observation that large supramolecular cargo, such as procollagen-I aggregates, traverse the Golgi without apparently leaving the lumen of the cisternae (Bonfanti et al., 1998; see also Volchuk et al. [2000] and other lines of evidence: Love et al., 1998; Lanoix et al., 2001; Martinez-Menárguez et al., 2001; Gilchrist et al., 2006; Glick and Luini, 2011). However, the central question, i.e., whether Golgi resident enzymes indeed recycle backward through the stack in synchrony with cisternal progression, and hence with cargo transport, remains undecided. Golgi cisternal maturation has been directly visualized in live yeast (Losev et al., 2006; Matsuura-Tokita et al., 2006;

R. Rizzo and S. Parashuraman contributed equally to this paper.

Correspondence to Alberto Luini: a.luini@ibp.cnr.it or luini@tigem.it

Abbreviations used in this paper: BFA, brefeldin A; GALT, β-1,4-galactosyltransferase; IF, immunofluorescence; LD, linear density; MANI, α-1,2-mannosidase IB; PM, plasma membrane; TGN, trans-Golgi network; VSV-G, vesicular stomatitis virus G protein.

The Rockefeller University Press $30.00
J. Cell Biol. Vol. 201 No. 7 1027–1036
www.jcb.org/cgi/doi/10.1083/jcb.201211147

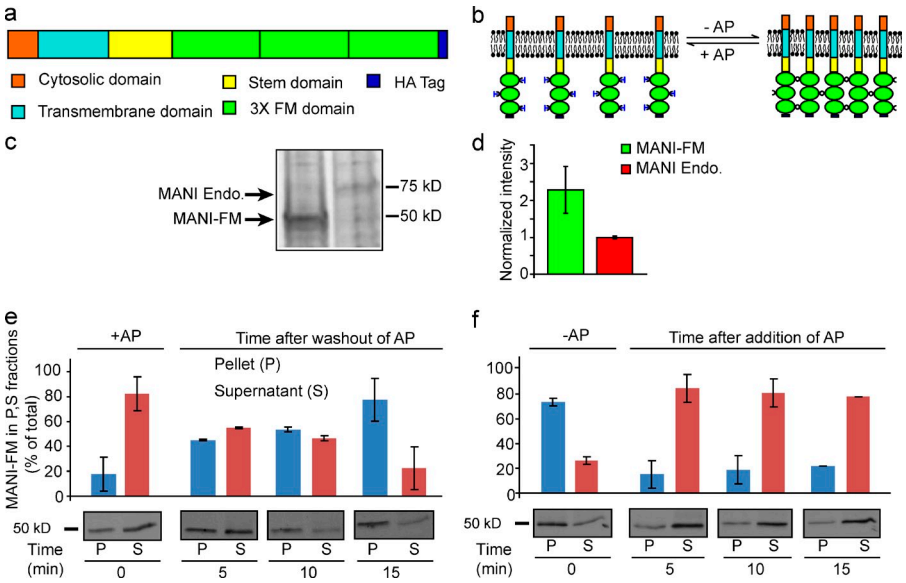

Figure 1. **Domain composition and reversible polymerization of MANI-FM.** (a) Three FM domains followed by an HA tag were fused to the C-terminal end of the Golgi-targeting portion (cytosolic, transmembrane, and luminal stem domains) of mouse MANI. (b) Scheme of MANI-FM polymerization and depolymerization in the absence and presence of AP. (c) To quantify the amount of MANI-FM present in the transfected cells relative to the endogenous protein, transfected HeLa cells were pulsed with radiolabeled amino acids for 24 h, and the endogenous and transfected proteins were immunoprecipitated and examined by autoradiography. Under the immunoprecipitation conditions most of the target proteins were immunoprecipitated. (d) Quantitation of the levels of MANI-FM relative to that of the MANI (c) suggest the levels of MANI-FM varied between two- and threefold that of the endogenous protein. (e) MANI-FM polymerization as revealed using a sedimentation assay. HeLa cells expressing MANI-FM were cultured in the presence of 1 µM AP, and then the AP was washed out for the indicated times before cell lysis and low-speed centrifugation to separate the pellet and supernatant fractions. The MANI-FM in these fractions was then quantified by gel electrophoresis and Western blotting. MANI-FM shifts from the supernatant to the pellet in <15 min. (f) MANI-FM depolymerization. HeLa cells expressing MANI-FM were washed out of AP 15 min (see panel e) and then 1 µM AP was added again to the cells for the indicated times. MANI-FM shifts back to the supernatant in <5 min. Data are mean ± SEM, from three independent experiments.

Emr et al., 2009), implying that Golgi residents do recycle in yeast; but no such evidence has so far been reported in mammals, possibly because of the insufficient resolution of current video microscopy technologies. This remains a stumbling block in the field, and, presumably because of the resulting uncertainties, a variety of different Golgi transport models have been proposed over the last few years (Patterson et al., 2008; Pfeffer, 2010; Mironov and Beznoussenko, 2012).

To overcome this block, we have devised an approach to monitor the intra-Golgi movements of Golgi residents at the resolution of EM. The approach is based on the engineering of Golgi resident constructs that can be reversibly polymerized. These constructs, when polymerized, are likely to become unable to enter recycling vesicles or tubules either because they are too large to enter the carriers and/or because they might be incompatible with the vesicular membrane curvature. We examined the transport behaviors of these constructs in their monomeric and polymeric states. The stable and the maturing cisternae models predict very different behaviors for monomers and polymers. According to the maturation model, Golgi residents maintain their position in the stack by recycling in synchrony with cisternal progression. This model thus predicts that if a suitably modified cis-Golgi resident protein is polymerized and prevented from entering Golgi carriers and hence from recycling, it will remain within the lumen of a cisterna and move to the trans side of the Golgi stack (Bonfanti et al., 1998). If the polymeric resident is then depolymerized once it arrives at the trans-Golgi, the resulting monomers should reenter vesicles and recycle back to the cis-Golgi at rates compatible with the maturation mechanism. In contrast, according to the stable cisternae models, a Golgi resident protein should localize at its level in the stack independent of its ability to enter Golgi carriers.

Our current results provide evidence that (a) polymerized Golgi residents are unable to enter Golgi carriers and (b) they move from the cis- to the trans-Golgi within the cisternal lumen. Thus, monomeric residents maintain their position in the Golgi by recycling through the stack in synchrony with the forward movement of cargo. These findings support the cisternal maturation mechanism in mammalian cells.

Results

Construction and characterization of reversibly polymerizable Golgi residents

To engineer a polymerizable Golgi resident, we fused the Golgi targeting portions (cytosolic tail, transmembrane domain, and stem region) of mouse α-1,2-mannosidase IB (MANI; Becker et al., 2000), a cis/medial Golgi enzyme (Dunphy and Rothman, 1983; Marra et al., 2001), with three tandem FM domains that dimerize spontaneously but can be dissociated by AP12998 (AP; Rivera et al., 2000) and with an HA tag for detection (MANI-FM; Fig. 1 a). Once polymerized, these constructs can generate large two-dimensional submembrane networks (Fig. 1 b). In addition, we prepared a similar construct using the targeting portions of the trans-Golgi enzyme β-1,4-galactosyltransferase (GALT-FM; Cole et al., 1996b).

We then expressed MANI-FM in HeLa cells (at levels that were two- to threefold higher than those of the endogenous Mannosidase I; see Fig. 1, c and d) and studied the polymerization/depolymerization kinetics of MANI-FM. For this, we used a sedimentation assay whereby polymers and monomers can be distinguished by their distribution in the pellet versus supernatant fractions, respectively (Volchuk et al., 2000). In the monomeric state (+AP), MANI-FM was in the supernatant, whereas after AP washout it shifted to the pellet, reflecting the formation of large MANI-FM polymers (Fig. 1 e). This shift started 5 min after AP washout and was complete by 15 min. Sucrose gradient centrifugation confirmed that MANI-FM shifts from a monomeric to a polymeric state within 15 min of AP removal

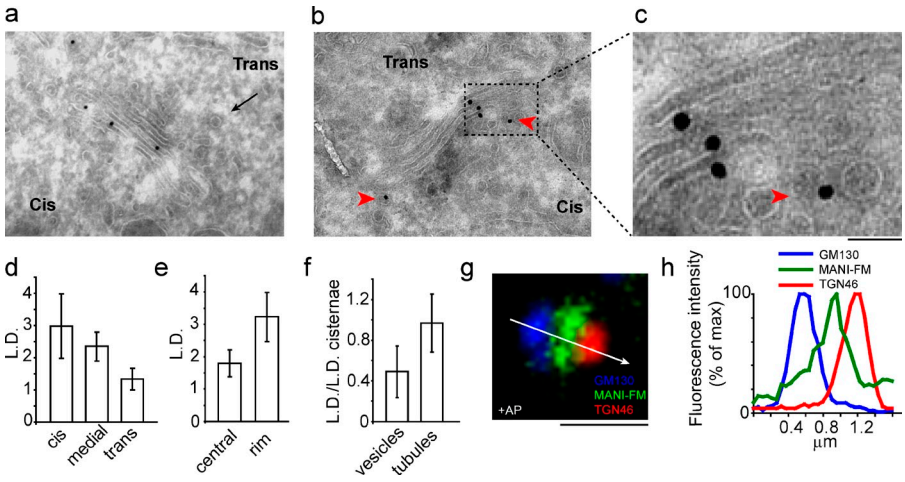

Figure 2. **MANI-FM localizes to a cis/medial position in the Golgi stack.** HeLa cells expressing MANI-FM were cultured in the presence of AP, and then fixed and processed for cryoimmunolabeling with an anti-HA antibody (10-nm gold particles). (a) Localization of MANI-FM in the cis-/medial cisternae, with a clathrin bud (arrow) marking the trans side. (b) An example of the preferential rim distribution of MANI-FM. (c) An enlargement of b, with MANI-FM in a peri-Golgi carrier (arrowhead). (d–f) Quantification of the distribution of MANI-FM across the stack (d), in the central versus the rim sections of the cisternae (e), and in peri-Golgi vesicles and tubules (f). Data are mean ± SEM, obtained from analyses of 28 stack profiles. (g) Localization of MANI-FM in a Golgi stack under confocal microscopy. MANI-FM (green) localizes between GM130 (blue) and TGN46 (red). The white arrow across the stack was used for line-scan analyses. The image is representative of >30 stacks analyzed. (h) Fluorescence intensity distribution of markers along the line scan (arrow in g). The fluorescence intensities were normalized to their respective peak values. The image and the corresponding quantitation are representative of at least 30 Golgi ministacks from three independent experiments. For this experiment, n = 30. Bars: (a) 270 nm; (b) 240 nm; (c) 60 nm; (g) 1 μm.

(unpublished data). We then added AP to polymeric MANI-FM (see Fig. 1 e) to induce depolymerization. MANI-FM shifted back to the supernatant rapidly (Fig. 1 f). Thus, MANI-FM polymerizes upon AP removal in ∼10–12 min and it depolymerizes with AP addition in <5 min.

Next, we sought to define suitable conditions to examine the intra-Golgi localization of MANI-FM in its monomeric or polymeric states (+AP). First, we used nocodazole, which fragments the Golgi complex into separate but structurally and functionally "normal" stacks (ministacks; Cole et al., 1996a; Trucco et al., 2004). The advantages of the ministacks are that (a) they provide good resolution between the cis-Golgi and the trans-Golgi by immunofluorescence (IF; Shima et al., 1997; Fig. S1, a–d); (b) they lack interstack tubular zones, which facilitates the analysis of peri-Golgi vesicles/tubules by EM (Trucco et al., 2004); and (c) they are physically isolated from other stacks, which rules out the possibility of exchange of cargo through contacts with adjacent stacks, like in the Golgi ribbon (Trucco et al., 2004; Pfeffer, 2010). Second, we emptied the ER of MANI-FM by cycloheximide treatment for 30 min before starting our observations to ensure that all of the MANI-FM that we examine was localized in the Golgi complex (see Materials and methods). Third, we sought to verify whether the targeting/retention mechanisms acting on MANI-FM (which contains the targeting motifs of the endogenous enzyme; see Fig. 1 a) are indeed similar in efficiency to those acting on the full-length protein. To this end, we compared the abilities of similar amounts of MANI-FM and full-length MANI to escape the Golgi and reach the plasma membrane (PM). In cells expressing low-medium levels of these two proteins, they localized only at the Golgi, whereas in highly expressing cells (∼20% of the cell population), the two constructs were both at the Golgi and the PM (see Materials and methods and Fig. S1, e–h). Thus, the Golgi targeting and retention properties of MANI-FM do not appear to differ considerably from those of the transfected full-length enzyme. Similar observations have been reported for other Golgi enzymes (Berger, 2002). In the localization experiments here, we included only cells expressing low-medium levels of MANI-FM (see Materials and methods).

Using these conditions, we assessed the distribution of monomeric MANI-FM (+AP) in Golgi cisternae and in peri-Golgi vesicles and tubules (as defined in Materials and methods) using immuno-EM and stereology. MANI-FM showed higher linear density (LD) in the cis- > medial > trans-cisternae, similar to the localization reported for the endogenous enzyme (Dunphy and Rothman, 1983; Marra et al., 2001; Fig. 2, a and d; and see also Fig. S3 a). Moreover, MANI-FM was more concentrated at the rims than in the central parts of the cisternae (Fig. 2, b, c, and e); it was present in vesicles and tubules at concentrations 50 and 96% of that in cisternae, respectively (tubules here include both dissociated carriers and inter-cisternal tubular connections; see Materials and methods; Fig. 2 f); and it was practically absent in the ER and in regions outside of the stack area, including the PM. By confocal microscopy, MANI-FM (again in cells expressing low-medium levels of the construct) localized between the cis-Golgi network and the trans-Golgi network (TGN; stained with the cis-Golgi network and TGN markers GM130 and TGN46, respectively), in qualitative agreement with the EM data (Fig. 2, g and h). This MANI-FM localization was similar to that of the full-length MANI, and it was also similar to that seen in the intact Golgi complex of NRK cells, where the cis-Golgi and trans-Golgi can be easily distinguished, even without nocodazole-mediated dissociation (unpublished data).

We also examined the localization of the GALT-FM construct. As monomers, GALT-FM localized in the trans- >> medial > cis-cisternae, as visualized by EM (Fig. S1 i) and by confocal microscopy (not depicted). Again, this represented a distribution that was similar to that of the corresponding endogenous enzyme (Teasdale et al., 1992).

Polymerization prevents the entry of Golgi MANI-FM into peri-Golgi carriers

We then polymerized MANI-FM by removing AP for 15 min, and examined the ability of the polymer to enter Golgi vesicular/tubular carriers. The concentration (as LD) of MANI-FM in vesicles and tubules dropped by ∼90%, to barely detectable levels (Fig. 3, a and b). Moreover, MANI-FM lost its concentration at

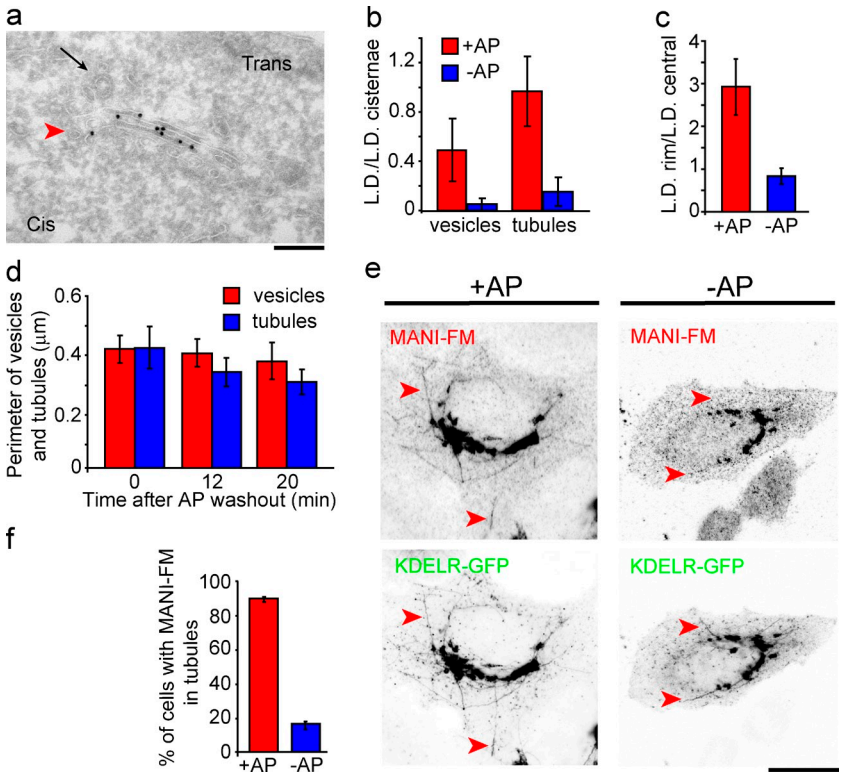

Figure 3. **Polymerization prevents MANI-FM entry into vesicles and tubules.** HeLa cells were transfected with MANI-FM in the presence of AP, and then deprived of AP for 15 min to induce polymerization. (a) Polymeric MANI-FM (−AP for 15 min) is nearly absent in Golgi vesicles (arrowhead) and tubules. The trans side of the stack was identified by clathrin-coated buds (arrow). (b) Quantification of MANI-FM in vesicles and tubules. Polymeric MANI-FM (−AP) is strongly depleted in vesicles and tubules compared with the monomer (+AP). (c) MANI-FM distribution along the cisternal length, expressed as the ratio between the LD in the rims versus the central part of the cisternae. MANI-FM shifts to a more central localization after polymerization. More than 20 stack profiles were analyzed for each condition. (d) The membrane length of vesicles and tubules, as a measure of the surface area, quantitated and expressed as perimeter (in micrometers) was not appreciably changed after polymerization of MANI-FM. The total surface area of tubules decreased by ∼25% after polymerization. (e) HeLa cells transfected with MANI-FM and KDEL receptor–GFP (KDELR-GFP) and kept in the presence or absence of AP (for 10 min) were treated with 6 µg/ml BFA for 8 min to induce tubules emanating from the Golgi, and then fixed and stained for MANI-FM. MANI-FM enters BFA-induced tubules in the presence of AP (monomers) but not in the absence of AP (polymers). (f) The number of BFA-induced tubules positive for MANI-FM was quantified. At least 10 cells per condition per experiment were analyzed, and the results are from three independent experiments. Data are means ± SEM. Bars: (a) 250 nm; (e, +AP) 15 µm; (e, −AP) 18 µm.

the rims of the Golgi cisternae and was distributed randomly along the cisternal length (Fig. 3 c and see also Fig. 5 c). The Golgi morphology and the number of peri-Golgi vesicles and tubules did not change except for a reduction (25%) in the surface area of the tubules (Fig. 3 d). We also examined the ability of polymerized MANI-FM to enter Golgi tubules induced by the toxin brefeldin A (BFA; Lippincott-Schwartz et al., 1990). These tubules have a diameter of 40 to 80 nm (Lippincott-Schwartz et al., 1990), which is similar to that of Golgi carriers and contain Golgi-resident proteins (Lippincott-Schwartz et al., 1990). An 8-min treatment with BFA induced the formation of numerous Golgi tubules containing either the cis-Golgi marker KDEL receptor (Fig. 3, e and f), the trans-Golgi marker galactosyltransferase, or the TGN marker TGN46 (not depicted). Polymeric MANI-FM did not enter these tubules, whereas MANI-FM monomers entered the tubules freely (Fig. 3, e and f). Polymeric MANI-FM also reduced the number of BFA-induced tubules by 30–40%. However, this reduction did not prevent the redistribution of the Golgi residents, including MANI-FM, into the ER after a 30-min exposure to BFA (Fig. S2, a–d). This is probably because of the peculiar mode of BFA-induced retrograde transport. As live-imaging experiments have shown (Sciaky et al., 1997), the addition of BFA leads to the formation of numerous tubules containing Golgi residents. When these tubules fuse with the ER they cause a sudden collapse of the Golgi into the ER in seconds (“blink out”), possibly caused by a tension-driven membrane flow (Sciaky et al., 1997). Such a complete collapse can presumably bring back to the ER even those proteins that do not actually enter the tubules. We also examined whether polymeric MANI-FM and GALT-FM can enter vesicular/tubular carriers derived from the ER (Bannykh and Balch, 1997; Antonny and Schekman, 2001). Both of these FM constructs were retained in the ER when expressed in the absence of AP, whereas after depolymerization (+AP), they left the ER and rapidly reached the Golgi complex (Fig. S2, e–h).

In sum, polymerization prevents MANI-FM from entering Golgi vesicles and tubules, including BFA-induced tubules and ER-derived tubular-vesicular carriers. This effect of polymerization might be because (a) the polymers are too large to enter the vesicles/tubules, (b) the polymers form a rigid platform that is incompatible with the curvature of the vesicles/tubules (Copic et al., 2012), or (c) the polymerization hides the sorting signals that allow MANI-FM to enter into vesicles/tubules. The inability of polymers to enter long BFA tubules and the preference of polymers for the flat areas of the cisternae over the rims favor the second of these three possibilities.

Polymerization causes MANI-FM to move forward in the Golgi stack

Finally, we sought to determine whether upon shifting from a monomeric to polymeric state MANI-FM remains in its cis position, as would be predicted by stable cisternae models, or it moves from cis- to trans-cisternae, as would be predicted by cisternal maturation. After AP removal (0 min), the MANI-FM peak shifted from the cis- to the medial cisternae (at 12 min), and then to the trans-cisterna (at 20 min; Fig. 4, a–e; and see also Fig. S3). Considering that polymerization lags behind by ∼10–12 min after AP washout (Fig. 1 e), the intra-Golgi transport

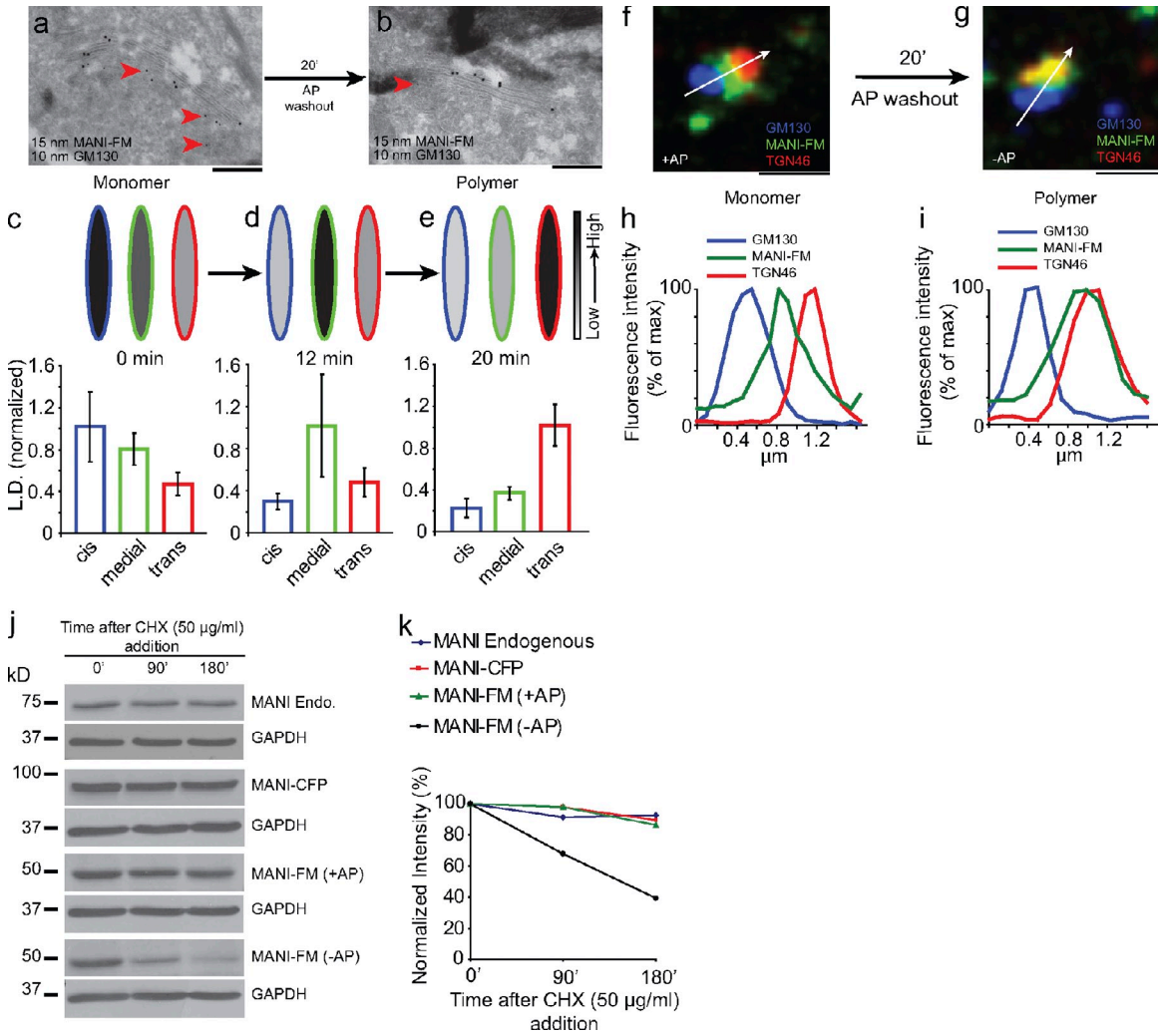

Figure 4. **Polymerized MANI-FM shifts from cis-/medial to trans-Golgi cisternae.** (a and b) HeLa cells were transfected with MANI-FM in the presence of AP (a), and then deprived of AP for 20 min (b) to induce polymerization. MANI-FM (15-nm gold) shifted from the cis-cisternae (labeled with the cis marker GM130; 10-nm gold; arrowheads) to the trans-cisternae after AP washout. (c–e) The distribution of MANI-FM across the stack at time 0 (c), 12 min (d), and 20 min (e) after AP washout, quantitated and expressed as LD normalized to that of the maximum. The normalized LD in the cis-cisternae is indicated in blue, in the medial in green, and in the trans in red. The schemes above the graph depict the shift of the MANI-FM peak from the cis/medial to the trans side of the stack. The intensities of the fill colors correspond to the normalized LD of the MANI-FM below (intensity scale on right). At least 20 stacks were analyzed for each time point. Data are mean ± SEM. (f–i) The shift of MANI-FM from the cis-/medial to the trans-Golgi was also visualized by confocal microscopy. HeLa cells were transfected with MANI-FM in the presence of AP (f), deprived of AP for 20 min (g), and then fixed and stained for MANI-FM (green), GM130 (blue), and TGN46 (red). The white arrow across the stacks was used for the line-scan analyses. The images are representative of >30 stacks analyzed for each condition. (h and i) Fluorescence intensity distribution of markers along the line scan (arrow in f and g). The fluorescent intensities were normalized to their respective peak values. The image and the corresponding quantitation are representative of at least 30 Golgi ministacks from three independent experiments. For this experiment, $n = 30$. (j) HeLa cells expressing MANI-FM or MANI-CFP cultured in the presence or absence of AP were treated with cycloheximide for the indicated times and the amount of protein was analyzed by lysing the cells followed by Western blotting. The quantification of the blots in panel j is shown in k. Whereas the polymeric MANI-FM (−AP) is degraded, the monomeric MANI-FM (+AP) is stable, like MANI-CFP and endogenous MANI. The results are typical of two independent experiments. Bars: (a and b) 220 nm; (f and g) 1 μm.

rate of polymeric MANI-FM was similar to that reported for procollagen and vesicular stomatitis virus G protein (VSV-G; Mironov et al., 2001), both of which have been proposed to move by cisternal maturation. A difficulty in interpreting these data (Fig. 4 d) is that according to the maturation model, 12 min after AP removal (MANI-FM polymerization), the cis-cisterna should be empty of MANI-FM, yet it appears to still contain measurable levels of this construct. This seeming discrepancy is most likely a result of the fact that the polymerization of MANI-FM is not instantaneous, but rather takes several minutes to reach completion after AP removal (Fig. 1 e). Hence, during this time interval, the residual monomeric MANI-FM fraction can recycle backward into the cis-cisterna. By light microscopy, the MANI-FM peak shifted away from GM130 (cis) and toward TGN46 (trans) within 20 min of AP removal, in agreement with the EM data (Fig. 4, f–i; and see also Fig. S4). Later, MANI-FM left the Golgi to assume a diffuse/punctate distribution (not depicted) and began to be degraded, presumably in the lysosomes (in contrast, the monomeric MANI-FM was as stable as the endogenous enzyme; Fig. 4, j and k).

We finally examined whether MANI-FM polymerization affects the morphology or the transport properties of the Golgi.

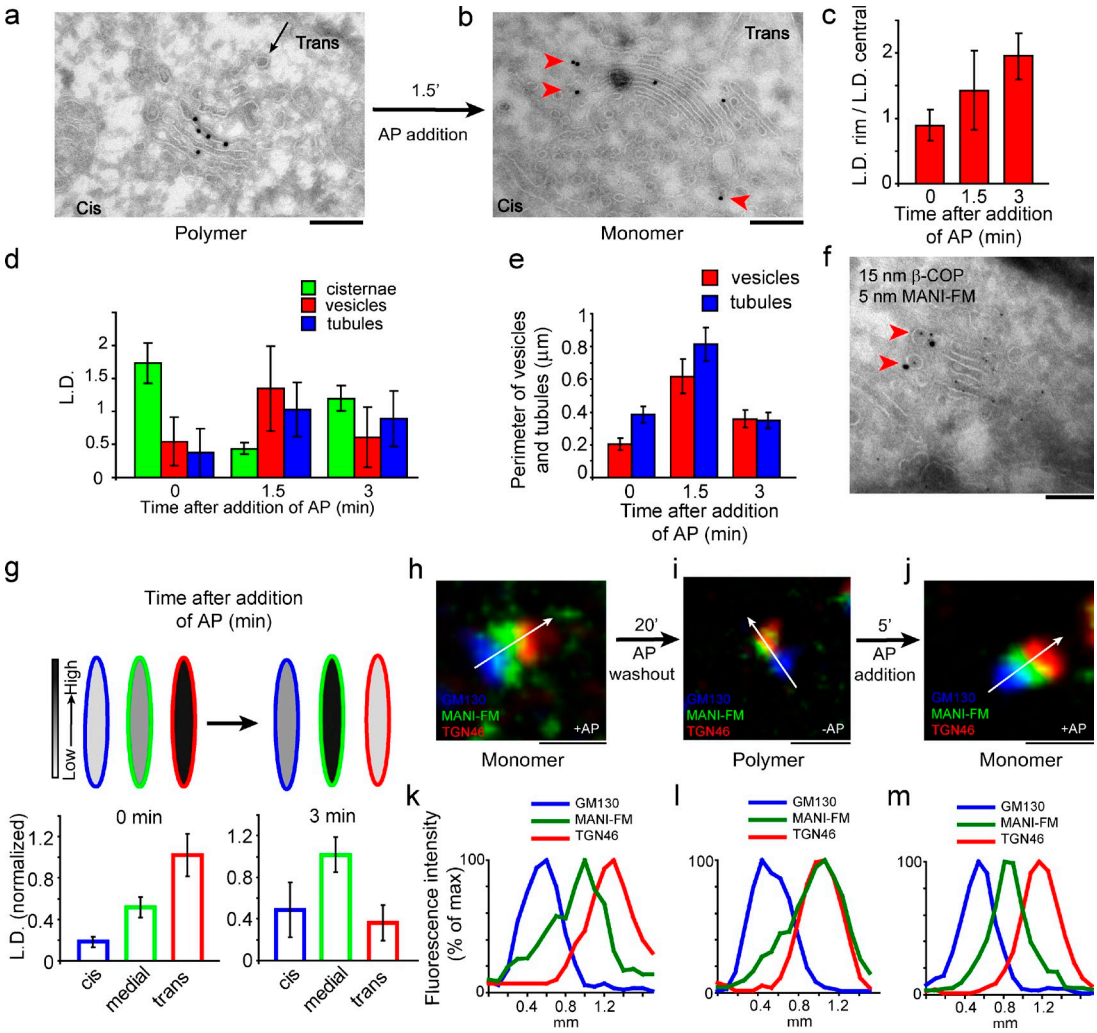

Figure 5. **MANI-FM recycles from the trans- to the cis-/medial Golgi after depolymerization in the trans-Golgi.** (a and b) HeLa cells were transfected with MANI-FM in the presence of AP and then deprived of AP for 20 min to induce polymerization and the transfer of MANI-FM to the trans-cisterna (a); finally, AP was added for 1.5 min (b). Arrowheads in b indicate the peri-Golgi carriers seen after AP addition. (c and d) The lateral distribution of MANI-FM along the cisternal length (c) and the distribution of MANI-FM in peri-Golgi carriers (d), expressed as LD. (e) The membrane length of vesicles and tubules as a measure of the surface area was quantitated and expressed as perimeter (in micrometers). (f) Colocalization of COPI and MANI-FM in vesicles and tubules (arrowheads) in cells fixed 1.5 min after addition of AP to depolymerize MANI-FM. (g) The change in distribution of MANI-FM from the trans- to the cis-/medial Golgi after addition of AP is expressed as LD normalized to that of the maximum (see Fig. 4 for description). Around 10–20 Golgi stack profiles were examined for each time point. Data are mean ± SEM. (h–m) The change in position of MANI-FM was also visualized under confocal microscopy. HeLa cells were fixed in the presence of AP (h and k), after 20 min of AP washout (i and l), and 5 min after readdition of AP (j and m). They were then stained for MANI-FM (green), GM130 (blue), and TGN46 (red). The white arrows across the stacks were used for line-scan analyses. Fluorescence intensity distribution of markers along the line scan (h–j, arrow), normalized to their respective peak values, is shown in k–m. The images are representative of >30 stacks analyzed for each condition from three independent experiments. For this experiment, n = 30. Bars: (a and b) 220 nm; (f) 120 nm; (h–j) 1 µm.

Several observations indicate that this is not the case: (a) transport of VSV-G into, through, and out of the Golgi complex and glycosylation of VSV-G occurred at normal rates after MANI-FM polymerization (Fig. S5, a–c); (b) polymerization of MANI-FM did not modify the morphology and the surface area of the Golgi apparatus both in the presence and absence of nocodazole (Fig. S5, d and e); and (c) the localization of the endogenous MANI was not affected by MANI-FM polymerization (Fig. S5, f and g). Thus, polymeric MANI-FM progresses from the cis- to the trans-Golgi without leaving the cisternae for vesicles/tubules at rates similar to those reported for procollagen and VSV-G (Mironov et al., 2001) and without perturbing the function and structure of the Golgi complex.

Depolymerization in the trans-Golgi restores the entry of MANI-FM into peri-Golgi carriers and causes MANI-FM to move back to its cis-/medial Golgi localization

The observation that MANI-FM moves forward in the stack when it is polymerized and is excluded from vesicular or tubular transport intermediates implies that monomeric MANI-FM normally recycles through these intermediates to maintain its cis-medial position. So far, however, direct evidence for recycling of Golgi residents through the stack in synchrony with transport in mammalian Golgi has been missing (Hoe et al., 1995; Malsam et al., 2005). We considered that if the MANI-FM polymers were depolymerized in the trans-cisterna, the resulting monomers

should regain their capability to enter carriers and could then recycle synchronously from the trans to the more proximal cisternae. To test this hypothesis, we first polymerized MANI-FM for 20 min to let the polymer reach the trans-cisterna (Fig. 4 e), and then we depolymerized the MANI-FM by adding back AP. At 20 min after AP washout, as expected, polymeric MANI-FM was homogeneously distributed in the trans-cisterna (Fig. 5 a; and see also Fig. 4 b). Upon depolymerization, MANI-FM rapidly (in 1.5–3 min) underwent the following distribution changes: (a) it became concentrated at the cisternal rims (Fig. 5 c); (b) it increased greatly in peri-Golgi vesicles/tubules (whose number also increased two- to threefold; Fig. 5, b, d, and e); and (c) it started to return back to the cis/medial localization that is typical of the MANI-FM monomers (Fig. 5, g–m). Throughout this redistribution process, the total levels of MANI-FM did not change detectably in the Golgi ministacks or in the ribbon, as assessed by MANI-FM fluorescence intensity at the Golgi (unpublished data). Notably, more than 50% of the MANI-FM–containing vesicles and tubules stained for COPI (Fig. 5 f and Fig. S5, n and o). Thus, the depolymerization of MANI-FM in the trans-cisterna appears to result in a burst of recycling mediated via COPI-dependent vesicles and tubules and in the rapid redistribution of MANI-FM to proximal cisternae. Even though the amount of the overexpressed MANI-FM is only two- to threefold that of the endogenous enzyme (Fig. 1 c), the sudden appearance of all of the cis/medial resident MANI-FM in the trans-cisterna can be presumably sensed and compensated for by mechanisms that actively respond to variable demands on the recycling process.

We also examined the structure of the Golgi carriers and of the Golgi stack by tomography. All reconstructions indicated that the morphology of the carriers (Fig. S5, h–m) and the structure and size of the Golgi stack were similar under all experimental conditions (Fig. S5, d and e). Moreover, tomography confirmed that most round, 50- to 80-nm structures were indeed vesicles (Fig. S5, h–m) and that the relative frequency of vesicles and tubules was similar to that seen in thin sections (not depicted).

Discussion

The main finding in this study is that although monomeric MANI-FM localizes to cis-medial Golgi cisternae and is present in peri-Golgi vesicles and tubules, the same construct, upon shifting to a polymeric state, moves from the rims to the center of the cisternae, disappears from peri-Golgi carriers, and moves from the cis-Golgi to the trans-Golgi cisternae at a rate reported for cisternal progression (Bonfanti et al., 1998). The simplest interpretation of these data are that monomeric MANI-FM normally recycles backward in the stack in lockstep with the progression of the cisternae (and of the cargo) via retrograde transport intermediates to maintain its cis location and that, when its recycling is inhibited by polymerization, it progresses through the stack along with the cisternal flow. Notably, monomeric MANI-FM mimics the localization, and hence presumably the behavior, of the corresponding endogenous resident enzyme. Alternative interpretations of the forward progression of MANI-FM polymers and, in particular, interpretations based on models by which cargo moves across stable cisternae via anterograde carriers must assume that polymerization induces MANI-FM to move forward in the stack by promoting its entry into anterograde transport intermediates. However, this is just the opposite of what is observed experimentally: polymerization induces a nearly complete disappearance of MANI-FM from all types of peri-Golgi carriers (both vesicles and tubules), as well as a shift of this construct from the rims to the center of the cisternae, a location that is not suitable for export. Another recently proposed stable cisternae model proposes that cargo moves forward by shifting across heterologous connected cisternae in adjacent stacks of the ribbon (Pfeffer, 2010). Also, this model is inconsistent with our results, which were obtained using physically separated ministacks. The findings in this study are therefore consistent with the cisternal progression maturation mechanism and not with stable cisternae models.

A further line of evidence in favor of cisternal maturation is that when MANI-FM is depolymerized in the trans-cisterna it rapidly reenters cisternal rims as well as vesicles/tubules and shifts back toward its cis-Golgi location. These data represent evidence for the rapid recycling of Golgi resident enzymes through the stack in mammals. Notably, a Golgi enzyme, GAlNacT2, has been recently reported to cycle rapidly between the Golgi and the intermediate compartment in mammals (Jarvela and Linstedt, 2012). This finding does not relate to the progression/maturation of the cisternae through the stack. Rather, it reflects the formation of new cis-cisternae from the intermediate compartment (Jarvela and Linstedt, 2012).

Regarding the mechanism of recycling, the MANI-FM–containing carriers that proliferate upon MANI-FM depolymerization appear to be COP-I–coated tubules and vesicles. Discordant conclusions have been proposed in the past regarding the question of whether vesicles or tubules (which might be dissociated or connected with adjacent cisternae) are involved in recycling (Orci et al., 2000; Lanoix et al., 2001; Martinez-Menárguez et al., 2001; Kweon et al., 2004; Trucco et al., 2004). Our current data, and the recent proposal that Golgi vesicles and tubules are strongly mechanistically related (Yang et al., 2011), might explain the previous discrepancies.

Do these findings show that cisternal maturation is the only mode of intra-Golgi transport? As is often stated in the literature, transport mechanisms are not mutually exclusive (Emr et al., 2009). Thus, although our data provide evidence for cisternal maturation, they do not exclude that other transport principles might coexist with the maturation process in the Golgi complex, such as vesicular trafficking (Rothman and Wieland, 1996; Malsam et al., 2005) or diffusional trafficking via continuities (Trucco et al., 2004), with the prevailing mechanism perhaps depending on the type of cargo being transported, the pathophysiological conditions, the cell type, and/or the trafficking step being examined. Examples of the eclectic nature of the transport apparatus have been provided by studies of the endocytic pathway, where different transport principles have been shown to coexist (Pryor and Luzio, 2009; De Matteis and Luini, 2011). Membrane trafficking has central roles in many cellular processes (Mellman and Warren, 2000; De Matteis and Luini, 2011). A better understanding of the full repertoire of eukaryotic trafficking principles will provide valuable insight into key aspects of cell physiology and pathology.

Materials and methods

Cell culture, constructs, antibodies, and reagents

HeLa cells were cultured in RPMI with 10% FCS and penicillin/streptomycin and NRK cells were cultured in DMEM with 10% FCS and penicillin/streptomycin. The mouse MANI fused to CFP and Rab1A-GFP were obtained from M.A. De Matteis (Telethon Institute of Genetics and Medicine, Naples, Italy; Marra et al., 2001; Venditti et al., 2012). The Golgi targeting portion of MANI (Becker et al., 2000) was PCR amplified and cloned into EcoRI and BamHI sites of pcDNA4B (Invitrogen). The construct containing three tandem FM domains was obtained from ARIAD Pharmaceuticals, and the FM domains were PCR amplified and cloned downstream of the mannosidase I Golgi targeting domains to obtain MANI-FM. To construct GALT-FM the same strategy was used where the Golgi-targeting portion of GALT (Cole et al., 1996b) was PCR amplified and cloned upstream of FM domains. The TGN46 antibody (used at 1:800 for IF) was obtained from AbD Serotec, the GM130 antibody (1:1,000 for IF and 1:50 for cryoimmunolabeling) from BD, HA monoclonal antibody (1:1,000 for IF and 1:300 for cryoimmunolabeling) from Covance, β-COP (1:20 for cryoimmunolabeling) from Thermo Fisher Scientific, anti–β-galactosyltransferase (1:400 for IF) from Sigma-Aldrich, anti–mannosidase I (1:100 for IF) from Sigma-Aldrich, anti–VSV-G polyclonal (1:8,000 for Western blotting) from Bethyl Laboratories, Inc., Alexa Fluor–conjugated second antibodies raised in donkey (Alexa Fluor 488, 568, and 633; 1:400 for IF) from Invitrogen, Dylight 405–conjugated donkey anti–mouse (1:100 for IF) from the Jackson Laboratory, and Protein A gold from Utrecht University. AP or DD solubilizer was obtained from ARIAD Pharmaceuticals or Takara Bio Inc., respectively. Endoglycosidase H was obtained from New England Biolabs, Inc. The protease inhibitor cocktail was purchased from Roche. Radiolabeled amino acids were purchased from PerkinElmer. All other reagents were obtained from Sigma-Aldrich.

Experimental conditions for MANI-FM polymerization

HeLa cells were transfected with the MANI-FM construct using Mirus transfection reagent following the manufacturer's instructions. After 24 h of transfection in the presence of 1 µM AP at 37°C, the media was changed and 1 µM of fresh AP was added for 30 min at 37°C. The cells were then treated with 33 µM nocodazole for 3 h in the presence of 1 µM AP, and 50 µM CHX was added for the last 30 min at 37°C. Importantly, the MANI-FM levels at the Golgi remained constant throughout this period. AP was then washed out of a subset of samples for the indicated times in the presence of CHX and nocodazole. All experiments were done in the presence of nocodazole and CHX unless otherwise indicated.

Radioactive labeling and immunoprecipitation

The method used was essentially as described previously (Bonifacino, 2001) with small modifications as described below. HeLa cells transfected with MANI-FM were cultured in the presence of AP for 12 h and then the media was substituted with one containing 0.05 mCi/ml of radiolabeled (^{35}S)cysteine and methionine and further cultured for 24 h in the presence of AP. The cells were then lysed in RIPA buffer (150 mM NaCl, 20 mM Tris, pH 8.0, 0.1% SDS, 0.5% sodium deoxycholate, and 1% Triton X-100) and immunoprecipitated with anti-MANI and anti-HA antibodies for 6 h at 4°C. The immunoprecipitate was resolved by SDS-PAGE followed by autoradiography. The intensity of the bands was quantitated using ImageJ.

MANI-FM sedimentation/polymerization assay

The sedimentation assay to reveal the polymerization status of MANI-FM was performed as described previously (Volchuk et al., 2000). In brief, after treatment, the cells were lysed in lysis buffer (1% Triton X-100, 20 mM Hepes, pH 7.4, 100 mM KCl, 2 mM EDTA, 1 mM DTT, and protease inhibitor cocktail from Roche) at 4°C for 30 min. The lysate was then centrifuged at 20,000 *g* for 10 min, and the pellet and supernatant fractions were separated and analyzed by SDS-PAGE and immunoblotting.

Immuno-EM: data acquisition and quantitation

The samples were fixed and prepared using standard methods, essentially as described previously (Mironov et al., 2001). In brief, the cells were fixed with 2% paraformaldehyde and 0.2% gluteraldehyde in PBS, for 2 h at room temperature (for cryoimmunolabeling), or with 4% paraformaldehyde and 0.05% gluteraldehyde, for 30 min at room temperature (for immunonanogold and gold enhancement labeling). For cryoimmunolabeling, the cells were then washed with PBS/0.02 M glycine, scraped in 12% gelatin in PBS, and then embedded in the same solution. The cells embedded in gelatin were cut in 1-mm blocks and infiltrated with 2.3 M sucrose at 4°C, mounted on aluminum pins, and frozen in liquid nitrogen. The samples were then sectioned and the ultrathin cryosections were picked up in a mixture of 50% sucrose and 50% methylcellulose and incubated with antibodies to antigen of interest followed by protein A gold. For immunonanogold the cells were permeabilized with 0.2% saponin in blocking solution (PBS containing 1% BSA and 50 mM NH_4Cl) and incubated with antibodies to antigen of interest in the same solution at 4°C for overnight, followed by second antibodies labeled with nanogold in the same solution for 2 h at room temperature. The gold particles were then enhanced by nanogold enhancer (Nanoprobes) according to the manufacturer's instructions. The samples were then epon embedded and ultra-thin sections (50–70 nm) were prepared. The samples were then examined under an iTEM microscope (JEOL Ltd.). Random sampling for the Golgi stacks was performed, with the only criterion for selection being the presence of gold label on Golgi stacks that were sectioned perpendicularly to the plane of cisternae. Stacks were imaged at a magnification of 20,000 or 30,000 using a Morada CCD camera using the iTEM image acquisition software (JEOL Ltd.). Some cells (~20% of the total) expressed high levels of MANI-FM and showed this construct at the PM. These cells were discarded. The cells selected for quantitation typically had 2–15 gold particles per stack. The images were analyzed using the iTEM image analysis platform (Olympus). The polarity of the stacks was assigned based on compositional and morphological criteria. The former was based on immunogold staining with antibodies anti-GM130, a cis-Golgi marker. The morphological criteria were based on the presence of clathrin buds or vesicles at the TGN side of the Golgi and of typical fenestrated cisternae (cis-Golgi). The clathrin buds/vesicles localized at the TGN at variable distances from the stack (from very close to up to 500 nm from the last trans-cisterna). Only those stacks where the association of clathrin buds to the trans side was unambiguous were considered for quantitation. The two criteria (morphological and compositional) were always in agreement. Several Golgi structures were evaluated. The number of cisternae varied from three to five. For quantitation, we classified them as cis, medial, or trans. Cis indicated the cis-most cisterna in the case of a stack with three or four cisternae, and the two cis-most cisternae in the case of a stack with five cisternae (here, the LD was the mean of the two). Trans was the last (trans) cisterna. Medial was the remaining one or two central cisternae. Vesicles were round profiles of 50–80 nm in diameter, present within 200 nm of the rims of the stack. Tubules were elongated profiles with length/width ratios greater than two. Of note, the analysis of thin sections precludes the discrimination of dissociated carriers and inter-cisternal tubular connections, and so quantification of tubules includes both of these. The cisternal rims were the most peripheral 100 nm of the cisternal profiles, and the rest of the cisterna was considered as the central cisternal part. All images were evaluated by three independent observers in a blind fashion. For surface density calculations, the number of gold particles associated with a structure was counted, and the membrane length was measured using the iTEM software. The density was then expressed as LD (number of gold particles/micrometer). When gold particles localized close to more than one structure, they were assigned to the closest structure. The number of Golgi stacks evaluated is specified in the legends.

EM tomography

The sample preparation and tomographic reconstruction was done essentially as described previously (Trucco et al., 2004). In brief, HeLa cells were fixed with 2% gluteraldehyde for 2 h at room temperature, and the samples were then processed, stained, dehydrated, and epon embedded. The samples were sectioned (200-nm sections), and gold particles were placed on the surface of the plastic sections and examined by an electron microscope (Tecnai-12; FEI). The Golgi profiles with well-preserved structures were identified and the images were acquired at tilt angles of +65° to −65° at 1° intervals, with a magnification of 26,500 using a Veletta CCD digital camera. The tomographic reconstruction was done using the Inspect 3D (FEI).

IF and confocal microscopy

Cells were fixed and immunostained as described previously (Trucco et al., 2004). In brief, the cells grown on coverslips were fixed with 4% paraformaldehyde for 10 min at room temperature and then permeabilized with 0.2% saponin in blocking solution (PBS containing 1% BSA and 50 mM NH_4Cl) followed by incubation with antibodies to antigen of interest in the same solution at 4°C overnight, followed by second antibodies labeled with Alexa Fluor dyes (Invitrogen). The coverslips were then mounted in the mounting media (16% [wt/vol] Mowiol 4–24 [EMD Millipore] and 30% [vol/vol] glycerol in PBS) and examined under a confocal microscope (LSM710; Carl Zeiss). The images were then acquired with a pinhole set to

1 and under nonsaturating conditions using a 63× objective (1.4 NA). The images were acquired using the Zen software system (Carl Zeiss). The line-scan analysis was performed as described previously (Dejgaard et al., 2007). In brief, images of stacks stained for GM130, TGN46, and MANI-FM were acquired with a pinhole set to 1 airy unit and under nonsaturating conditions, and these were analyzed by the Zen image analysis platform. Only cells with a moderate level of expression were considered for the analysis. Cells that expressed high levels of the MANI-FM construct, leading to a localization of the protein in the PM (~20% of the cells), were avoided. Golgi stacks with clearly separated GM130- and TGN46-stained zones were identified and used for the analysis. A line was drawn in the middle of the stacks along the cis–trans direction, and the fluorescence intensity of each stained marker along this line was plotted. The images obtained were then processed using Metamorph 7.7.3.0 (Universal Imaging), with the "Image with Zoom" function for presentation. At least 30 stacks were examined per treatment and a representative image is shown. For the computational coalescence of line scans, the normalized line scans (normalization of distances was done by considering the start of the GM130 peak as 0 and the end of the TGN peak as 1) to be coalesced were plotted together and coalesced using the Gaussian curve fitting option of GraphPad Prism version 5.0 software.

Endoglycosidase H assay

HeLa cells transfected with MANI-FM were infected with VSV (VSV-ts045), incubated at 40°C for 3 h, and transferred to 32°C for the indicated times. The cells were then lysed in RIPA buffer (150 mM NaCl, 20 mM Tris, pH 8.0, 0.1% SDS, 0.5% sodium deoxycholate, and 1% Triton X-100) at 4°C for 30 min. The lysates were clarified by centrifugation at 14,000 rpm for 10 min. The supernatants were treated with Endoglycosidase H in the EndoH buffer (0.05 M sodium citrate, pH 5.5) at 37°C overnight. The treated samples were then resolved by SDS-PAGE and Western blotting was done using anti–VSV-G antibody.

Online supplemental material

Fig. S1 shows the FM fusion proteins localize mainly to the Golgi and have appropriate sub-Golgi localizations. Fig. S2 shows that the polymerization of FM fusion proteins does not prevent their BFA-induced retrograde transport to ER but prevents their exit out of the ER. In Fig. S3, the frequency distribution analysis and double immunolabeling with GM130 as cis marker confirms that polymerization of MANI-FM induces its shift from the cis to trans side. Fig. S4 shows the shift of polymeric MANI-FM from cis- to trans-Golgi as visualized by confocal microscopy. Fig. S5 shows that polymerization of MANI-FM does not affect the morphology or the functioning of the Golgi. Online supplemental material is available at http://www.jcb.org/cgi/content/full/jcb.201211147/DC1.

We thank R. Polishchuk, A. De Matteis, D. Corda, G. Griffiths, M. Lowe, J. Cancino, and G. D'Angelo for valuable discussions and R. Hegde for help with computational coalescence.

We thank the Italian ministry of University and Research, Telethon Institute of Genetics and Medicine, and Associazione Italiana per la Ricerca sul Cancro for financial support. We thank the microscopy facility at the Instituto di Biochimica delle Proteine and Institute of Genetics and Biophysics/Consiglio Nazionale delle Richerch for technical assistance. We also thank ARIAD pharmaceuticals for sharing the FM constructs and AP12998.

Author contributions: R. Rizzo was involved in the planning and execution of the experiments. S. Parashuraman was involved in the planning and execution of the experiments and in the writing of the paper. P. Mirabelli contributed to the execution of experiments. C. Puri helped in the execution of the immuno-EM experiments. J. Lucocq was involved in the analysis of EM data. A. Luini was involved in the writing of the paper and in the overall direction of the project.

Submitted: 27 November 2012
Accepted: 9 May 2013

References

Antonny, B., and R. Schekman. 2001. ER export: public transportation by the COPII coach. *Curr. Opin. Cell Biol.* 13:438–443. http://dx.doi.org/10.1016/S0955-0674(00)00234-9

Bannykh, S.I., and W.E. Balch. 1997. Membrane dynamics at the endoplasmic reticulum–Golgi interface. *J. Cell Biol.* 138:1–4. http://dx.doi.org/10.1083/jcb.138.1.1

Becker, B., A. Haggarty, P.A. Romero, T. Poon, and A. Herscovics. 2000. The transmembrane domain of murine alpha-mannosidase IB is a major determinant of Golgi localization. *Eur. J. Cell Biol.* 79:986–992. http://dx.doi.org/10.1078/0171-9335-00127

Berger, E.G. 2002. Ectopic localizations of Golgi glycosyltransferases. *Glycobiology*. 12:29R–36R. http://dx.doi.org/10.1093/glycob/12.2.29R

Bonfanti, L., A.A. Mironov Jr., J.A. Martínez-Menárguez, O. Martella, A. Fusella, M. Baldassarre, R. Buccione, H.J. Geuze, A.A. Mironov, and A. Luini. 1998. Procollagen traverses the Golgi stack without leaving the lumen of cisternae: evidence for cisternal maturation. *Cell*. 95:993–1003. http://dx.doi.org/10.1016/S0092-8674(00)81723-7

Bonifacino, J.S. 2001. Metabolic labeling with amino acids. *Curr. Protoc. Mol. Biol.* Chapter 10:Unit 10.18.

Cole, N.B., N. Sciaky, A. Marotta, J. Song, and J. Lippincott-Schwartz. 1996a. Golgi dispersal during microtubule disruption: regeneration of Golgi stacks at peripheral endoplasmic reticulum exit sites. *Mol. Biol. Cell*. 7:631–650.

Cole, N.B., C.L. Smith, N. Sciaky, M. Terasaki, M. Edidin, and J. Lippincott-Schwartz. 1996b. Diffusional mobility of Golgi proteins in membranes of living cells. *Science*. 273:797–801. http://dx.doi.org/10.1126/science.273.5276.797

Copic, A., C.F. Latham, M.A. Horlbeck, J.G. D'Arcangelo, and E.A. Miller. 2012. ER cargo properties specify a requirement for COPII coat rigidity mediated by Sec13p. *Science*. 335:1359–1362. http://dx.doi.org/10.1126/science.1215909

De Matteis, M.A., and A. Luini. 2011. Mendelian disorders of membrane trafficking. *N. Engl. J. Med.* 365:927–938. http://dx.doi.org/10.1056/NEJMra0910494

Dejgaard, S.Y., A. Murshid, K.M. Dee, and J.F. Presley. 2007. Confocal microscopy-based linescan methodologies for intra-Golgi localization of proteins. *J. Histochem. Cytochem.* 55:709–719. http://dx.doi.org/10.1369/jhc.6A7090.2007

Dunphy, W.G., and J.E. Rothman. 1983. Compartmentation of asparagine-linked oligosaccharide processing in the Golgi apparatus. *J. Cell Biol.* 97:270–275. http://dx.doi.org/10.1083/jcb.97.1.270

Emr, S., B.S. Glick, A.D. Linstedt, J. Lippincott-Schwartz, A. Luini, V. Malhotra, B.J. Marsh, A. Nakano, S.R. Pfeffer, C. Rabouille, et al. 2009. Journeys through the Golgi—taking stock in a new era. *J. Cell Biol.* 187:449–453. http://dx.doi.org/10.1083/jcb.200909011

Gilchrist, A., C.E. Au, J. Hiding, A.W. Bell, J. Fernandez-Rodriguez, S. Lesimple, H. Nagaya, L. Roy, S.J. Gosline, M. Hallett, et al. 2006. Quantitative proteomics analysis of the secretory pathway. *Cell*. 127:1265–1281. http://dx.doi.org/10.1016/j.cell.2006.10.036

Glick, B.S., and A. Luini. 2011. Models for Golgi traffic: a critical assessment. *Cold Spring Harb. Perspect. Biol.* 3:a005215. http://dx.doi.org/10.1101/cshperspect.a005215

Hoe, M.H., P. Slusarewicz, T. Misteli, R. Watson, and G. Warren. 1995. Evidence for recycling of the resident medial/trans Golgi enzyme, N-acetylglucosaminyltransferase I, in ldlD cells. *J. Biol. Chem.* 270:25057–25063. http://dx.doi.org/10.1074/jbc.270.42.25057

Jarvela, T., and A.D. Linstedt. 2012. Irradiation-induced protein inactivation reveals Golgi enzyme cycling to cell periphery. *J. Cell Sci.* 125:973–980. http://dx.doi.org/10.1242/jcs.094441

Kweon, H.S., G.V. Beznoussenko, M. Micaroni, R.S. Polishchuk, A. Trucco, O. Martella, D. Di Giandomenico, P. Marra, A. Fusella, A. Di Pentima, et al. 2004. Golgi enzymes are enriched in perforated zones of Golgi cisternae but are depleted in COPI vesicles. *Mol. Biol. Cell*. 15:4710–4724. http://dx.doi.org/10.1091/mbc.E03-12-0881

Lanoix, J., J. Ouwendijk, A. Stark, E. Szafer, D. Cassel, K. Dejgaard, M. Weiss, and T. Nilsson. 2001. Sorting of Golgi resident proteins into different subpopulations of COPI vesicles: a role for ArfGAP1. *J. Cell Biol.* 155:1199–1212. http://dx.doi.org/10.1083/jcb.200108017

Lippincott-Schwartz, J., J.G. Donaldson, A. Schweizer, E.G. Berger, H.P. Hauri, L.C. Yuan, and R.D. Klausner. 1990. Microtubule-dependent retrograde transport of proteins into the ER in the presence of brefeldin A suggests an ER recycling pathway. *Cell*. 60:821–836. http://dx.doi.org/10.1016/0092-8674(90)90096-W

Losev, E., C.A. Reinke, J. Jellen, D.E. Strongin, B.J. Bevis, and B.S. Glick. 2006. Golgi maturation visualized in living yeast. *Nature*. 441:1002–1006. http://dx.doi.org/10.1038/nature04717

Love, H.D., C.C. Lin, C.S. Short, and J. Ostermann. 1998. Isolation of functional Golgi-derived vesicles with a possible role in retrograde transport. *J. Cell Biol.* 140:541–551. http://dx.doi.org/10.1083/jcb.140.3.541

Malsam, J., A. Satoh, L. Pelletier, and G. Warren. 2005. Golgin tethers define subpopulations of COPI vesicles. *Science*. 307:1095–1098. http://dx.doi.org/10.1126/science.1108061

Marra, P., T. Maffucci, T. Daniele, G.D. Tullio, Y. Ikehara, E.K. Chan, A. Luini, G. Beznoussenko, A. Mironov, and M.A. De Matteis. 2001. The GM130 and GRASP65 Golgi proteins cycle through and define a subdomain of the intermediate compartment. *Nat. Cell Biol.* 3:1101–1113. http://dx.doi.org/10.1038/ncb1201-1101

Martinez-Menárguez, J.A., R. Prekeris, V.M. Oorschot, R. Scheller, J.W. Slot, H.J. Geuze, and J. Klumperman. 2001. Peri-Golgi vesicles contain retrograde but not anterograde proteins consistent with the cisternal progression model of intra-Golgi transport. *J. Cell Biol.* 155:1213–1224. http://dx.doi.org/10.1083/jcb.200108029

Matsuura-Tokita, K., M. Takeuchi, A. Ichihara, K. Mikuriya, and A. Nakano. 2006. Live imaging of yeast Golgi cisternal maturation. *Nature*. 441:1007–1010. http://dx.doi.org/10.1038/nature04737

Mellman, I., and G. Warren. 2000. The road taken: past and future foundations of membrane traffic. *Cell*. 100:99–112. http://dx.doi.org/10.1016/S0092-8674(00)81687-6

Mironov, A.A., and G.V. Beznoussenko. 2012. The kiss-and-run model of intra-Golgi transport. *Int. J. Mol. Sci.* 13:6800–6819. http://dx.doi.org/10.3390/ijms13066800

Mironov, A.A., G.V. Beznoussenko, P. Nicoziani, O. Martella, A. Trucco, H.S. Kweon, D. Di Giandomenico, R.S. Polishchuk, A. Fusella, P. Lupetti, et al. 2001. Small cargo proteins and large aggregates can traverse the Golgi by a common mechanism without leaving the lumen of cisternae. *J. Cell Biol.* 155:1225–1238. http://dx.doi.org/10.1083/jcb.200108073

Nakano, A., and A. Luini. 2010. Passage through the Golgi. *Curr. Opin. Cell Biol.* 22:471–478. http://dx.doi.org/10.1016/j.ceb.2010.05.003

Orci, L., M. Amherdt, M. Ravazzola, A. Perrelet, and J.E. Rothman. 2000. Exclusion of golgi residents from transport vesicles budding from Golgi cisternae in intact cells. *J. Cell Biol.* 150:1263–1270. http://dx.doi.org/10.1083/jcb.150.6.1263

Patterson, G.H., K. Hirschberg, R.S. Polishchuk, D. Gerlich, R.D. Phair, and J. Lippincott-Schwartz. 2008. Transport through the Golgi apparatus by rapid partitioning within a two-phase membrane system. *Cell*. 133:1055–1067. http://dx.doi.org/10.1016/j.cell.2008.04.044

Pfeffer, S.R. 2007. Unsolved mysteries in membrane traffic. *Annu. Rev. Biochem.* 76:629–645. http://dx.doi.org/10.1146/annurev.biochem.76.061705.130002

Pfeffer, S.R. 2010. How the Golgi works: a cisternal progenitor model. *Proc. Natl. Acad. Sci. USA*. 107:19614–19618. http://dx.doi.org/10.1073/pnas.1011016107

Pryor, P.R., and J.P. Luzio. 2009. Delivery of endocytosed membrane proteins to the lysosome. *Biochim. Biophys. Acta*. 1793:615–624. http://dx.doi.org/10.1016/j.bbamcr.2008.12.022

Rivera, V.M., X. Wang, S. Wardwell, N.L. Courage, A. Volchuk, T. Keenan, D.A. Holt, M. Gilman, L. Orci, F. Cerasoli Jr., et al. 2000. Regulation of protein secretion through controlled aggregation in the endoplasmic reticulum. *Science*. 287:826–830. http://dx.doi.org/10.1126/science.287.5454.826

Rothman, J.E., and F.T. Wieland. 1996. Protein sorting by transport vesicles. *Science*. 272:227–234. http://dx.doi.org/10.1126/science.272.5259.227

Sciaky, N., J. Presley, C. Smith, K.J. Zaal, N. Cole, J.E. Moreira, M. Terasaki, E. Siggia, and J. Lippincott-Schwartz. 1997. Golgi tubule traffic and the effects of brefeldin A visualized in living cells. *J. Cell Biol.* 139:1137–1155. http://dx.doi.org/10.1083/jcb.139.5.1137

Shima, D.T., K. Haldar, R. Pepperkok, R. Watson, and G. Warren. 1997. Partitioning of the Golgi apparatus during mitosis in living HeLa cells. *J. Cell Biol.* 137:1211–1228. http://dx.doi.org/10.1083/jcb.137.6.1211

Teasdale, R.D., G. D'Agostaro, and P.A. Gleeson. 1992. The signal for Golgi retention of bovine beta 1,4-galactosyltransferase is in the transmembrane domain. *J. Biol. Chem.* 267:4084–4096.

Trucco, A., R.S. Polishchuk, O. Martella, A. Di Pentima, A. Fusella, D. Di Giandomenico, E. San Pietro, G.V. Beznoussenko, E.V. Polishchuk, M. Baldassarre, et al. 2004. Secretory traffic triggers the formation of tubular continuities across Golgi sub-compartments. *Nat. Cell Biol.* 6:1071–1081. http://dx.doi.org/10.1038/ncb1180

Venditti, R., T. Scanu, M. Santoro, G. Di Tullio, A. Spaar, R. Gaibisso, G.V. Beznoussenko, A.A. Mironov, A. Mironov Jr., L. Zelante, et al. 2012. Sedlin controls the ER export of procollagen by regulating the Sar1 cycle. *Science*. 337:1668–1672. http://dx.doi.org/10.1126/science.1224947

Volchuk, A., M. Amherdt, M. Ravazzola, B. Brügger, V.M. Rivera, T. Clackson, A. Perrelet, T.H. Söllner, J.E. Rothman, and L. Orci. 2000. Megavesicles implicated in the rapid transport of intracisternal aggregates across the Golgi stack. *Cell*. 102:335–348. http://dx.doi.org/10.1016/S0092-8674(00)00039-8

Yang, J.S., C. Valente, R.S. Polishchuk, G. Turacchio, E. Layre, D.B. Moody, C.C. Leslie, M.H. Gelb, W.J. Brown, D. Corda, et al. 2011. COPI acts in both vesicular and tubular transport. *Nat. Cell Biol.* 13:996–1003. http://dx.doi.org/10.1038/ncb2273